The Curious Case of 2-Propyl-1H-benzimidazole in the Solid State

DOI:
10.1021/acs.jpca.7b05220

Document Version
Accepted author manuscript

THE JOURNAL OF
PHYSICAL CHEMISTRY A

The Curious Case of 2-Propyl-1*H*-Benzimidazole in the Solid State: An Experimental and Theoretical Study

María Mar Quesada-Moreno,[†] Aurora J. Cruz-Cabeza,[‡] Juan Ramón Avilés-Moreno,[§] Pilar Cabildo,[¶] Rosa M. Claramunt,*[,¶] Ibon Alkorta,[⫽] José Elguero,[⫽] Francisco J. Zúñiga,*[,^] and Juan Jesús López-González*[,†]

[†] Departamento de Química Física y Analítica, Universidad de Jaén, Campus Las Lagunillas, E-23071, Jaén, Spain
[‡] School of Chemical Engineering and Analytical Sciences, The University of Manchester, The Mill, Sackville Street, Manchester M13 9PL, United Kingdom
[§] Departamento de Sistemas Físicos, Químicos y Naturales, Universidad Pablo de Olavide, E-41013, Sevilla, Spain
[¶] Facultad de Ciencias, Dpto. Química Orgánica y Bio-Orgánica, Universidad Nacional de Educación a Distancia (UNED), Senda del Rey 9, E-28040 Madrid, Spain
[⫽] Instituto de Química Médica, Centro de Química Orgánica Manuel Lora-Tamayo, CSIC, Juan de la Cierva 3, E-28006 Madrid, Spain
[^] Facultad de Ciencia y Tecnología, Dpto. Física Materia Condensada, Universidad del País Vasco, Apdo. 644, E-48080 Bilbao, Spain

S *Supporting Information*

ABSTRACT: 2-Propyl-1*H*-benzimidazole (**2PrBzIm**) is a small molecule, commercially available, which displays a curious behavior in the solid state. **2PrBzIm,** although devoid of chirality, by fast rotation about a single bond of the propyl group in solution, crystallizes as a conglomerate showing chiroptical properties. An exhaustive analysis of its crystal structure and a wide range of experiments monitored by VCD spectroscopy have eliminated all possibilities of an artifact. What remains is a new example of the unexplained phenomenon of persistent supramolecular chirality.

---

1. INTRODUCTION

Azoles (imidazole, pyrazole, both triazoles and tetrazole) and benzazoles (benzimidazole, indazole and benzotriazole) when unsubstituted on the N atom possess one hydrogen-bond donor, the N–H (HBD), and at least one hydrogen-bond acceptor (HBA), the "pyridine-like" N atom. In the presence of other donors and acceptors or solvent molecules (e.g. water, methanol…), predicting the supramolecular chemistry displayed by these molecules may be challenging. In the absence of other donors and acceptors, however, hydrogen bonding (HB) in these compounds involves either catemeric (chain) or cyclic (ring) motifs. In previous studies we have reported the synthesis and

determination of crystal structures of 1*H*-benzimidazoles,[1,2,3] 1*H*-indazoles,[3,4,5,6,7] and 1*H*-benzotriazoles[3,8,9]. The many possible hydrogen bonding networks for these compounds observed in the solid state have been summarized in Scheme 1.

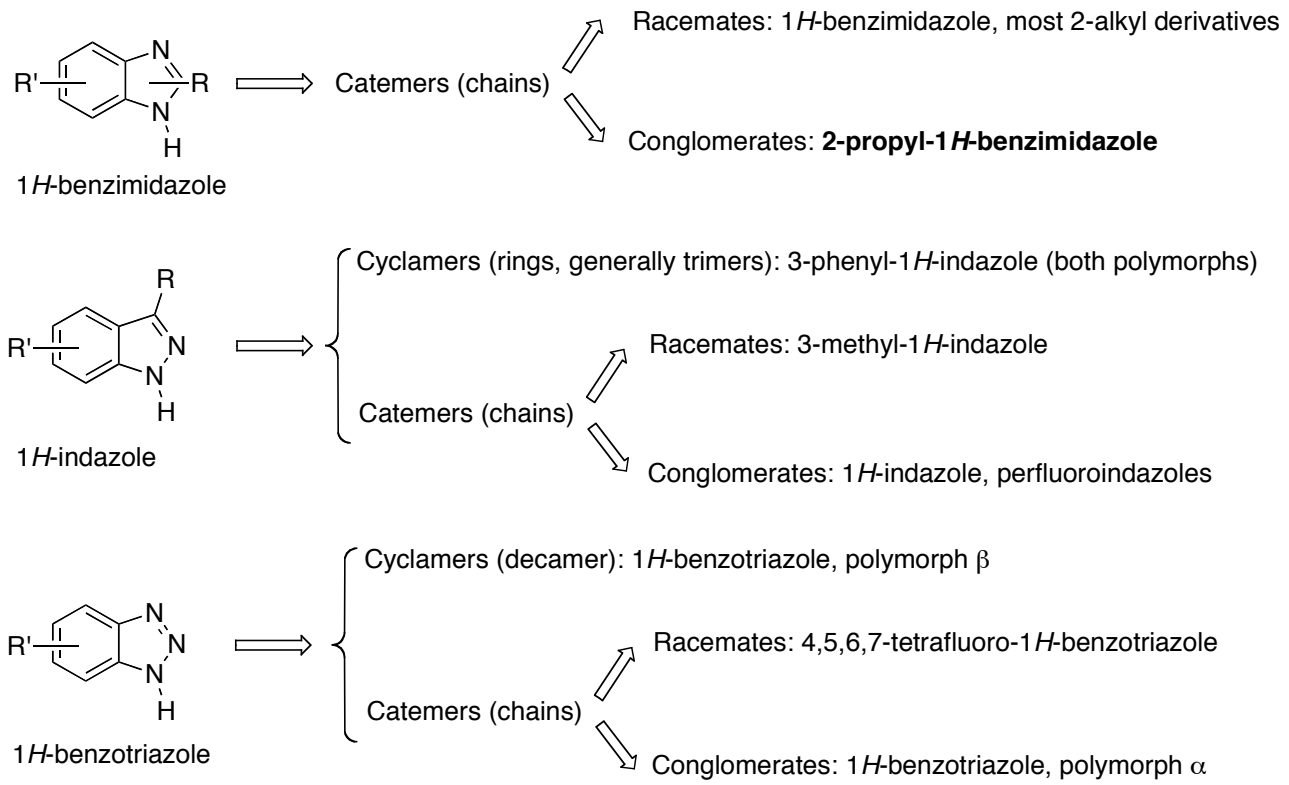

Scheme 1. The different HB networks found in benzazoles crystal structures.

In what refers to the chirality of the benzazoles crystal structures, we noticed that derivatives presenting catemeric motifs can display supramolecular chirality, therefore these compounds crystallize in either racemic crystals or enantiopure crystal structures in the form of conglomerates. It is expected that these conglomerates will have a 50:50 ratio of both enantiomeric crystals unless there is some chiral impurity present in the crystallizations. In this context, we found a very particular behavior in 2-propyl-1*H*-benzimidazole (**2PrBzIm). 2PrBzIm** is expected to crystallize as a 50:50 conglomerate (no chiral response) in the absence of chiral impurities,[10] however it is always obtained displaying a chiral response no matter the synthesis or crystallization method employed. In fact, various commercial samples, synthesized samples and recrystallized samples all displayed identical chiral responses despite the fact that no chiral compounds were present in any of the experiments. This unexpected result prompted us to study the structure and the chiral properties of this **2PrBzIm** in the gas-phase, solution and in the solid state using a combination of experimental and theoretical techniques including X-ray diffraction, non sensitive (IR and Raman) and sensitive (VCD) to chirality vibrational spectroscopies and various DFT calculations.

2. EXPERIMENTAL AND THEORETICAL METHODS

2.1 Sample preparation.

It was reported by Cuccia *et al*. that most commercial samples of conglomerate crystals are scalemic, *i.e*. with enantiomeric excess ranging from 3% to >90%.[11,12] The same happens for all samples of **2PrBzIm** we purchased from Aldrich at different times. The methods we have used to obtain suitable crystals being an essential part of this manuscript are described in section 3.4.

2.2. Experimental Methods: IR, Raman and VCD.

The IR and VCD spectra of **2PrBzIm** in $CDCl_3$ solution (liquid phase) and fluorolube and nujol mulls (solid phase) were recorded at room temperature using a JASCO FVS-4000 FTIR spectrometer, equipped with MCT (2000-900 cm^{-1}) detector. For the preparation of the emulsions, a few milligrams of the different samples of the analyzed crystals of **2PrBzIm** were mixed with fluorolube or nujol mineral oils in order to get suitable mulls. Special attention is needed when working with solid samples in circular dichroism spectroscopy.[13,14,15] In fact, we have measured the mulls in several positions by rotating the sample around both the beam propagation axes (90º and 180º) and that perpendicular to them (180º) with the purpose to get the true VCD peaks and to be sure on the absence of artifacts in the recorded VCD spectra.[13,14] The spectra were recorded using a standard cell equipped with BaF_2 and KBr windows, a resolution of 4 cm^{-1} and 8000 scans in blocks of 2000 scans (2000 scans for each orientation) in the case of mulls spectra and 8 cm^{-1} of resolution, 2000 scans and path lengths of 100 μm for solution spectra. Concerning the baseline correction, we have substracted the $CDCl_3$, nujol or fluorolube signals to the VCD spectra.

The IR spectrum of the solid sample obtained without any stirring from 3:1 Cl_2CH_2/hexane solvent mixture was recorded in the 2000-150 cm^{-1} region, with 300-400 scans and 2 cm^{-1} resolution, using the Bruker Vertex 70 spectrometer available in our laboratory in Jaen. The Pt ATR accessory (single reflection diamond ATR accessory) and the silicon beam-splitter were employed for the Far-IR region.

We also used a Bruker PMA50 optical bench coupled to a Vertex 70 spectrometer, equipped with a MCT detector available at the University of Malaga. The VCD spectrum in fluorolube mull was also recorded using a cell with KBr windows, a resolution of 4 cm^{-1} and 8000 scans.

2.3. Computational Methods.

All calculations were performed using GAUSSIAN09[16] at the M06-2X[17]/6-31G(d,p)[18] level of theory. The asymmetric unit of the **2PrBzIm** crystal structure was then optimized with the same models and using periodic boundary conditions in two directions, both corresponding to the two perpendicular hydrogen-bonded chain directions (along a and b). For this, two translation vectors were defined along a and b (x and y) equivalent to the experimental unit cell parameters a/b. Following the PBC optimization, the optimized PBC-geometries were used to derive dimer, tetramer and octamer models. These models were then used as input for frequency calculations from which calculated IR and VCR spectra were derived. Calculated frequencies were scaled by 0.947 in the case of the mid region and 0.966 for the far one.[19]

For the monomer calculations in the gas-phase, the rotatable bonds on the propyl chain were constraint to the experimental torsion values they have in the crystal structure and all other parameters were allowed to optimize. Various DFT models were used for the optimization of the two conformers including: M062X/6-31G(d,p), M062X/aug-cc-pVTZ and M062X/aug-cc-pVTZ in the presence of an SMD solvation model for benzene and water.

3. RESULTS AND DISCUSSION

3.1. Molecular and crystal structure of 2PrBzIm

2PrBzIm in the planar form is an achiral molecule that may adopt two configurations (Figure 1): *syn* [with the N(1)H proton on the same side of the propyl chain] and *anti* [with the N(1)H proton on the opposite side of the propyl chain, *i.e.* close to N3]. These configurations (*syn* and *anti*) can interconvert either via rotation about the C1-C2 bond or by a proton transfer through a tautomerization reaction, from N1 to N3 (Figure 1).

The relative stability of these configurations was computed using a DFT model (M062X/aug-cc-pVTZ) in three different media: i) in the gas-phase, ii) in benzene and iii) in water (Table 1). The *anti* configuration has lower energy in the gas-phase and in benzene but it is almost isoenergetic to the *syn* configuration in water. From 104 crystal structures of benzimidazoles in the Cambridge Structure Database,[20] it was found that 58% of them exhibit *anti* configurations versus a 42% of *syn* configurations. Both configurations are, therefore, equally accessible in the solid state and of very similar stability.

Figure 1. The *syn* and *anti* configurations of **2PrBzIm**.

Table 1. Relative stability of the *anti* and *syn* configurations of **2PrBzIm** as computed with various methods. Energy units in kJ·mol^{-1}.

Method	Solvation [a]	*Anti*	*Syn*
M062X/aug-cc-pVTZ	Gas	0.0	3.0
M062X/aug-cc-pVTZ	Benzene	0.0	2.4
M062X/aug-cc-pVTZ	Water	0.7	0.0

[a] SMD solvation model. Single point calculation on the gas-phase optimized geometries.

2PrBzIm has conformational chirality in the crystal without having any stereogenic center and the molecules of **2PrBzIm** exhibit *syn* configurations with deviations from planarity via rotation through the C1-C2 bond of about 45°. This kind of chirality is called "planar chirality" and uses as CIP stereodescriptors R_p and S_p,[21] but it is usually reserved for enantiomers that can be separated, i.e. having high barriers of enantiomerization (for the first examples of planar chiral organic benzimidazoles related to [2.2]paracyclophanes see reference 22). In solution, due to the low rotational barriers about the C1-C2 single bond, our model compound is expected to be oscillating about the planar configurations.

The crystal structure of **2PrBzIm** is orthorhombic $P2_12_12_1$, $Z = 16$, $Z' = 4$, with a pseudo-tetragonal cell (CSD refcode OHUZUO). The four independent molecules interact through N(1)-

H···N3' hydrogen bonds forming two independent and perpendicular (90º rotated) hydrogen bonded chains (Figure 2).

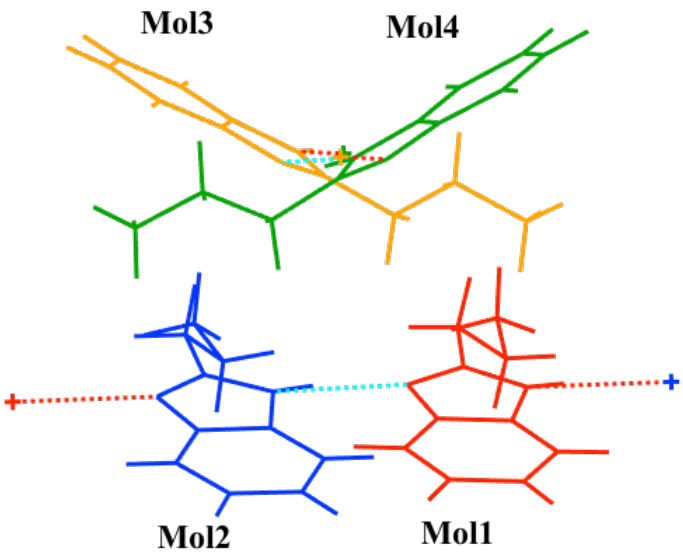

Figure 2. The four independent molecules of **2PrBzIm** (Mol1 to Mol4) in the crystal structure form two perpendicular HB chains. Independent molecules are color-coded. Dashed lines denote intermolecular H bonds.

Consecutive independent molecules along the chains exhibit conformations approximately related by glide plane symmetry resulting a V-shape pattern (Figure 2). The conformational torsion angles of the terminal propyl in consecutive molecules alternate between positive and negative values [45.5(3)º, –45.3(3)º and 44.3(3), –45.0(3)º]. The individual N-H dipoles of the molecules along the chain sum up, resulting in a larger net dipole that confers a polar character to the chains (see Figure 3). Note that the polarity of the chains could be inverted if the protons jump towards the acceptor N3 atoms. remember that the complete crystal is non polar.

Figure 3. A tetramer of one chain of **2PrBzIm**. Arrows represent the dipoles associated with the N-H bonds and dashed lines are hydrogen bonds.

Chains propagating along [010] direction are parallel-packed along [100] and form a double-layer together with chains symmetry related by one of the twofold screw axis of the space group. Another similar double-layer contains chains propagating along [100] direction and parallel-packed along the [010] direction. These double-layer slabs are stacked along [001] direction, forming a helicoidal (4_1 or 4_3 pseudo-symmetry) assembly of polar chains, as shown in Figure 4.

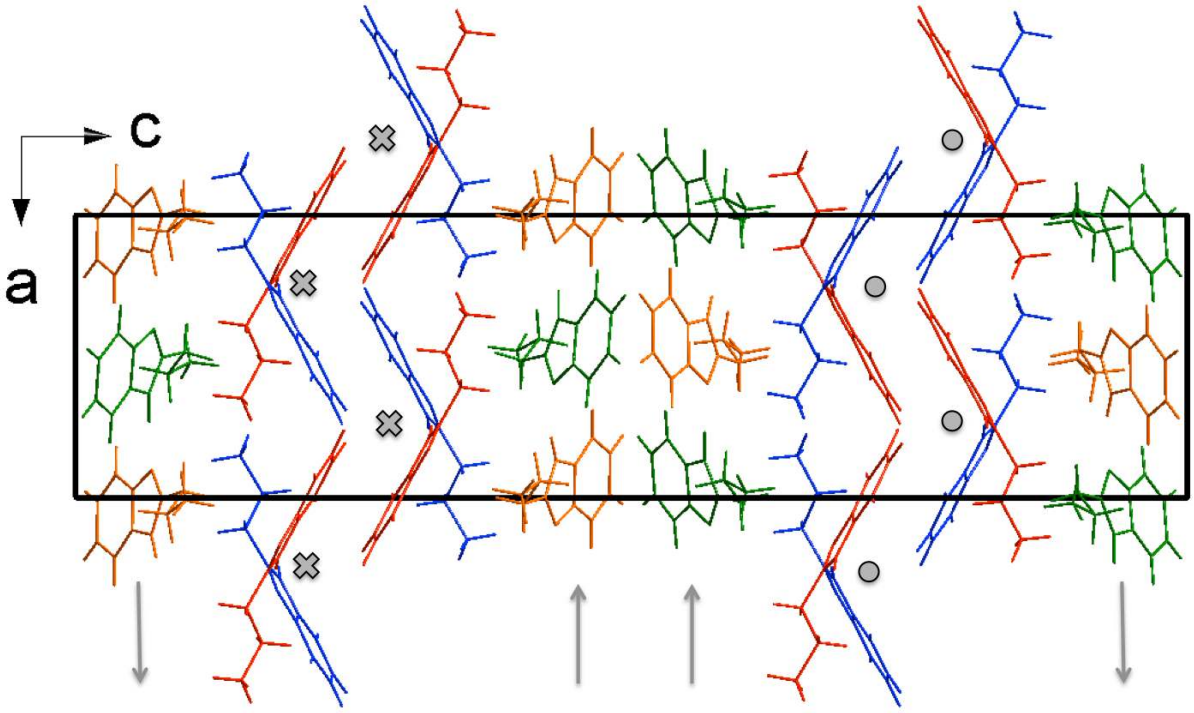

Figure 4. Slabs of molecular chains stacked along [001] direction. Slabs contain dipolar chains helicoidally arranged as stacked along the **c** direction. The arrows, dots (up) and crosses (down) indicate the polarity of the chains.

The local pseudo-symmetries of second kind operate intermolecularly relating pairs of molecules with opposite chirality giving rise to achiral molecular chains. These pseudo-symmetries, combined with the screw axis of the space group, generate polar achiral structural units built up with double-layers of chains. These units are three-dimensional objects with the same two-dimensional periodicity (**a**,**b**) of the crystal, and exhibit symmetry properties that could be approximated by the layer group $pb2_1a$. Consecutive slabs stacked along **c** are related by another local pseudo-symmetry 4_1 building up the crystal as a sequence of layer with the same symmetry but in alternated orientation $pb2_1a$ and $p2_1ab$ respectively (the same symmetry but 90º rotated around the **c** direction). We have noticed that the symmetry operation stacking slabs does not belong to the space group of the crystal, neither the (100) and (010)-glide planes relating adjacent molecules in the chains.

As a way of simplifying the crystallographic problem, we can analyze the pseudo-symmetry of the $P2_12_12_1$ crystal structure of **2PrBzIm** as two interpenetrated sub-structures (Figure 5). Each sub-structure is composed of $pb2_1a$ and $p2_1ab$ units combined with the remaining 2_1 axis of the space group. By imposing a higher symmetry to these substructures, space groups Pcab and Pbca can be imposed with maximal deviations of 0.131 Å and 0.123 Å respectively. The space groups of the sub-structures are the same but with different settings and origins (SI). The complete structure

projected in Figure 4 corresponds to the superposition of the left and right sub-structures of Figure 5, whose space group symmetry is $P2_12_12_1$ - the intersection of the space groups Pcab and Pbca.

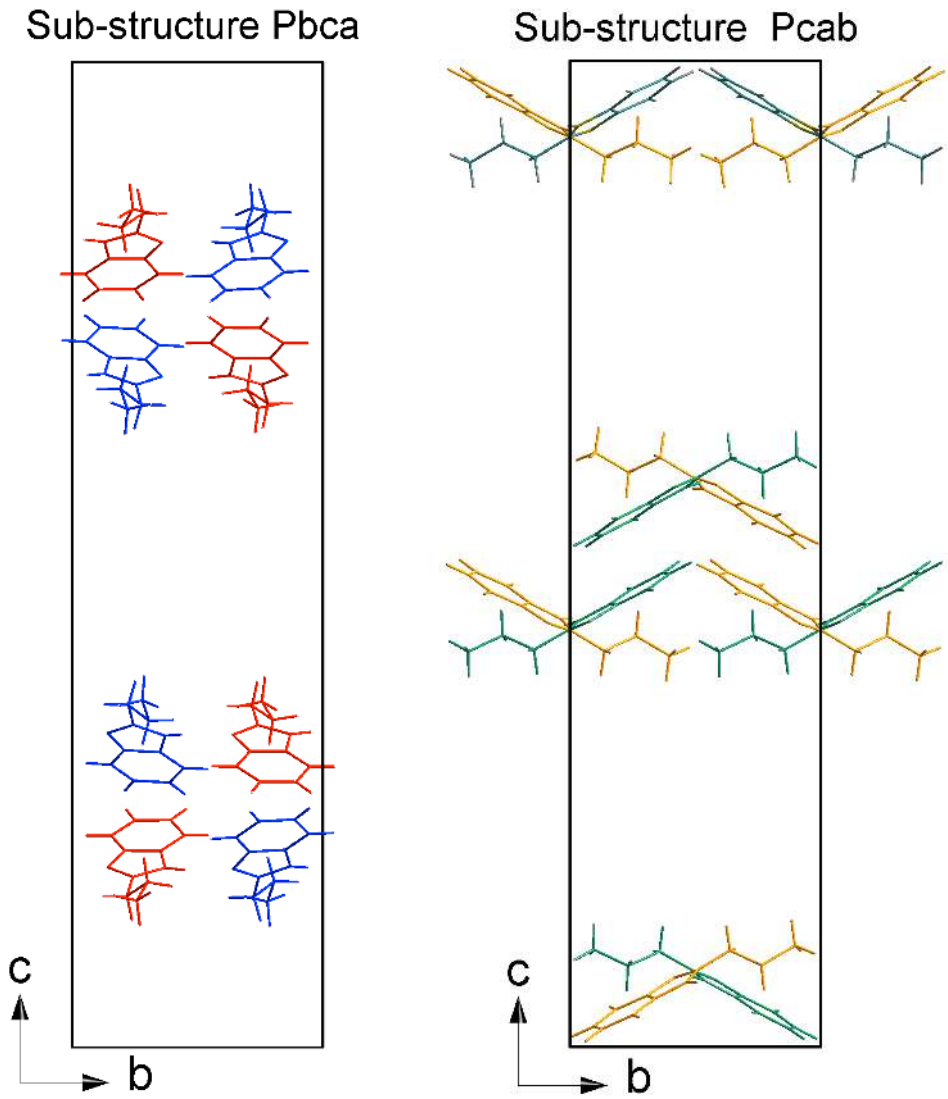

Figure 5. Substructures containing molecules Mol1 and Mol2 (left) and molecules Mol3 and Mol4 (right).

Note that a rotation of 180º around the **c**-direction, applied to any of the sub-structures prior to the superimposition, results in the same structure but described in a different way. Sub-structure Pbca and Pcab can be combined in three non-trivial different ways. First by superimposition of models shown in Figure 5, resulting in the structure of Figure 4 and the pattern of coordinates given in the published cif-file (CSD refcode OHUZUO); this structure will be referred as structure of reference (A). Two other ways consist in applying a rotation {C2z| ½,0,0} (Seitz notation) on one or in the other sub-structure, and then apply the superposition on the other, obtaining different sets of coordinates named models B and C. It can be observed that these new structural models correspond to different descriptions of the same structure. This can be easily proved using the crystallographic tool COMPUSTRU provided by the Bilbao Crystallographic Center[23] (details of the results are given in the SI). The transformations between the models A-B and A-C do not preserve the chirality and differ in an origin shift (0,0,1/2). When they are applied to the structure of

reference A, another equivalent set of coordinates are obtained. Actually, the transformation corresponds to one of the symmetry operations of the Euclidean normalizer $P4_2/mmc$ of the $P2_12_12_1$ space group in the case of special metric a = b ≠ c.[24] Another generator (1/4-y, 1/4-x, 1/4-z) would give rise to an equivalent set of coordinates preserving the chirality of the structure.

The local symmetries in the crystal can be considered as partial operations in the sense used for the description of order-disorder structures of equivalent layers. A quantitative study of the deviation from pseudo-symmetry in **2PrBzIm** has been undertaken refining several structural models where the four independent molecules are symmetry restricted by these local operations. Three models were tested. The first one (I) constraining the two independent molecules along the chains by a transformation approximated to glide planes $\{\sigma_x|1/2,1/2,0\}$ and $\{\sigma_y|1/2,0,0\}$ respectively, that is, two independent molecules in the crystal, one for each chain. Another model (II) with consecutive double layers of chains (slabs) related by a transformation approximated to a pseudo 4_1-screw axis, that is, two independent molecules in the unique independent slab. The third model (III) includes both pseudo-operations acting on one independent molecule. All the refinement performed with the JANA-2006[25] program where based on the same X-ray diffraction data reported in reference 3. The rotations and translations of the local operations relating rigid-body molecules were allowed to relax from the ideal values of the local symmetries. The resulting molecular parameters giving the orientation of the second molecule generated from the independent one by the pseudo-symmetry operations are summarized in Table 2.

Table 2. **Molecular parameters of the second position symmetry related by pseudo-symmetry in three different models. The asymmetric unit contains four independent molecules labeled Mol1 and Mol2 in one chain and, Mol3 and Mol4 in the other chain. In (I), molecules Mol2 and Mol4 are related by glide planes to Mol1 and Mol3 respectively. In (II) a pseudo-fourfold screw axis expands along the c direction the double-layer slabs containing Mol1 and Mol2. In (III), both local pseudo-symmetries applied to one molecule (Mol1) expand into the four independent molecules in the crystal. The pseudo-symmetries are introduced in the form of proper (1) or improper (-1) rotations (º) ϕ(z), χ(y) and φ(x) and translations (relative units) T_x, T_y and T_z. The reliability R-factor indicates the agreement of the structural models to the experimental data.**

	I-glide planes		**II-fourfold screw axis**		**III-glide-planes**		
	Mol. 2 (–1)	Mol. 4 (–1)	Mol. 3 (1)	Mol. 4 (1)	Mol. 2 (1)	Mol. 3 (–1)	Mol. 4 (1)
ϕ(z)	–0.01(4)	–179.23(6)	–88.15(4)	–91.12(4)	–88.11(4)	–0.02(4)	–91.13(4)
χ(y)	0.18(3)	–3.603(2)	–0.10(3)	0.014(3)	–0.08(3)	0.03(3)	0.42(3)
φ(x)	–183.15(6)	180.296(2)	–4.50(6)	1.81(6)	–4.66(6)	–183.13(7)	178.84(7)
T_x	0.0157(2)	–0.4971(2)	–0.2380(2)	0.2440(2)	–0.2373(1)	0.0153(1)	0.2587(1)
T_y	–0.4961(2)	0.0005(2)	–0.2350(2)	0.2452(2)	–0.2355(1)	–0.4965(1)	–0.2518(1)
T_z	0.00044(4)	0.00044(4)	–0.2491(1)	–0.2500(1)	–0.2489(1)	0.0005(1)	–0.2498(1)
R_{obs}	4.35		4.36		4.65		

It can be seen in Table 2 that the local operations significantly deviate from crystallographic mirror glide-plane (improper rotation close to 180º) and fourfold rotation, with translations located in positions shifted from rational values 1/4 and 1/2 as correspond to crystallographic glide planes and fourfold screw axis operations. The R-factors agreement reached in the refinements is close to the value R = 3.4 obtained in the refinement with four independent molecules, and confirms the high pseudo-symmetry exhibited by the molecular arrangement in this crystal.

Additionally, the comparison between the conformations of the four independent molecules can be done using the Mercury program.[26] Consecutive molecules in the chains are nearly superimposed (without flexibility) with displacements within 0.1006 Å and 0.0456 Å rmsd, that is, conformations of the enantiomers are essentially indistinguishable.

The results described above lead to classify the structure of **2PrBzIm** as a kryptoracemate, a chiral crystal structure formed from a racemate. The crystal structure is described in an Schonke space group and contains an equimolar mix of enantiomeric molecules. The molecules in the asymmetric unit ($Z' = 4$) are distributed into two pairs of enantiomers; each one with enantiomers related by a transformation that approximates a glide-plan. It has been pointed out,[27,28] that classification of a crystal structure as kryptoracemate may be wrong because a misunderstanding in the symmetry, and such warning has been taken very seriously. Although the results of the structural refinement (R-factor, anisotropic thermal displacements, correlations, etc.) do not point to any anomaly it is true that, in the present case, the pseudo-symmetries can play tricks. First, the crystals are twinned; in the reported structure a crystal with two pseudo-merohedral twin fragments related by a four-fold axis was measured. On the other hand, the determination of the absolute structure results ambiguous. However, the exhaustive analysis of the hidden pseudo-symmetries developed above may be enough to clear any doubts to skeptics. Moreover, the chiral character of the crystal has been sufficiently proved by means of VCD experiments demonstrating in any case the absence of inversion center in the structure.

3.2. On the origin of the chirality.

In the previous section, we have described the crystal structure of **2PzBzIm** as being built up from achiral supramolecular elements (chains) arranged in two sub-structures with symmetries close to centrosymmetric space groups (Pcab and Pbca). Where can we find then the origin of the chirality? Only the helical arrangement of the polar chains has all the features to display chirality. The N-H bonds confer a polar character to the molecular chains with spatial disposition related to a 4_1-helicoidal axis. We note that clockwise (*P*) and counter-clockwise (*M*) helicoidal arrangements can be interconverted by an inversion center, but also by inverting the polarity of one of the two independent chains through a proton transfer.

The chirality hypothesis presented above has been checked against theoretical calculations of the IR and VCD spectra that could be compared with the experimental ones in the solid state (powder, nujol or fluorolube mulls). For this, we built four different molecular models as depicted in Figure 6. Model-1 is just a monomer, Model-4 a tetramer of the hydrogen-bonded chain, Model-2x2 two dimers of two perpendicular chains and Model-4x2x2 one chain tetramer and two chain dimers oriented in perpendicular direction to the tetramer (Figure 3). Geometry optimizations, followed by IR and VCD calculations, of the models in Figure 6 were performed as described in the methods section. Whilst Model-1 was simply optimized in the gas-phase, Model-4 was optimized using periodic boundary conditions (PBC) in one direction and Models 2x2x2 and 4x2x2 were

optimized using PBC in two directions. Because of the possibility of tautomerization, all models were re-optimized and spectra recalculated after migrating the proton on N1 to N3 (Figure 1). Since the results obtained for models with the hydrogen atom on N1 were in better agreement with the experimental observations and the X-ray single crystal structure also confirmed the position of the proton on the N1 nitrogen (configuration *syn*), only the results for the main tautomer are given here.

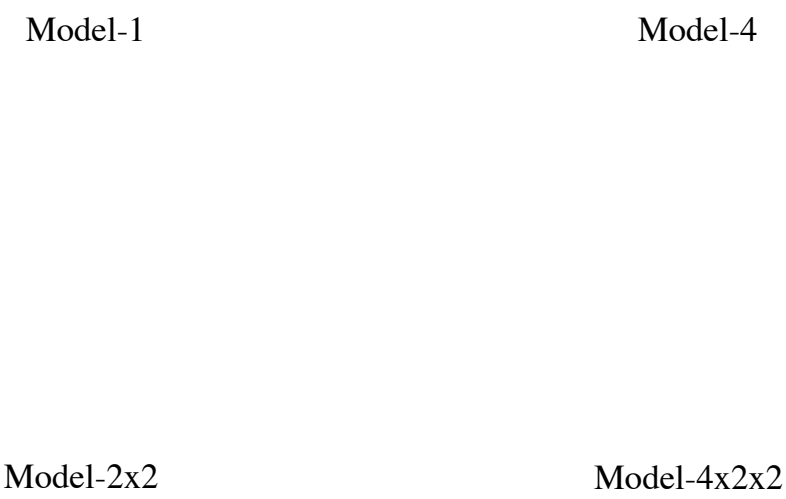

Figure 6. Molecular models used for the calculations of IR and VCD spectra.

In Figure 7, we compare experimental and computationally generated IR and VCD spectra. For the IR spectra, all models reproduced the experimental spectra fairly well except for the single monomer model (Model-1). At the far-IR end, where intermolecular interactions may partly influence the lower modes, we observe the best agreement with the most sophisticated Model 4x2x2 (see Figure 8). The predicted VCD spectra were more sensitive to the theoretical model employed. Here, the monomer and the single chain models (Models 1 and 4) performed quite poorly. Only when the stack of two chains is included in the model, it starts to be a better correspondence between the experimental and the theoretical VCD spectra (Figure 7 and 3.3. section).

The crystallization of achiral molecules in chiral crystals is not uncommon. Dryzun and Avnir[29] report that 32% of crystals in the Cambridge Structural Database[20] are chiral crystals. Of those, 57% consist of molecules that are achiral but adopt homochiral "frozen" conformers when crystallized.[29] By far, the most common cases of achiral molecules crystallizing in chiral crystals involve chiral conformations. **2PrBzIm** could indeed adopt chiral conformations through rotation of bonds about the propyl chain. As explained above, the conformations of **2PrBzIm** deviate from planarity by ~ +45° as well as –45° (due to local pseudo-symmetries) therefore both chiral conformers are present in the crystal in equal amounts which should result in no chiral response due to conformation. The origin of the chirality does not lie on the conformation, nor on the hydrogen-bonded chain, which runs parallel to a chiral 2_1 axis.

The origin of the chirality in this structure relates to the packing of the hydrogen-bonded chains as it is schematically represented in Figure 9. A double layer of hydrogen-bonded chains pointing to the right can pack over perpendicular chains pointing into the plane or out of the plane. This subtle difference in the packing differentiates the enantiomeric crystals. Understandably, then, it is not surprising that the predicted VCD spectra starts resembling the experimental one more significantly only when the packing of the chains is included in the models.

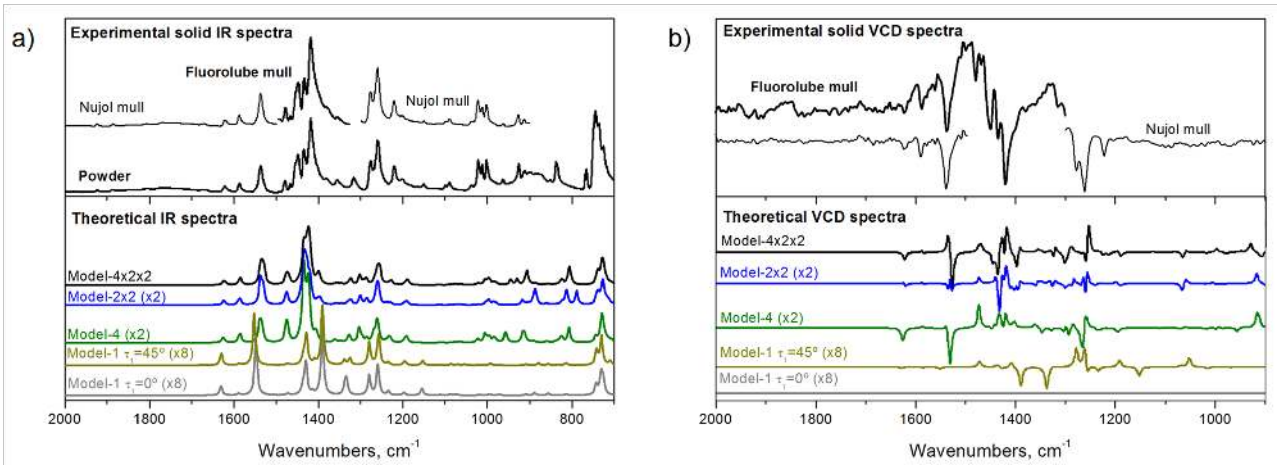

Figure 7. Experimental (upper) and predicted (lower) scaled IR (a) and VCD (b) spectra of **2PrBzIm**. Upper: Experimental IR spectrum of the powder sample and IR-VCD spectra in fluorolube and nujol mulls. Lower: IR and VCD theoretical spectra of Model-4x2x2 (black), Model-2x2 (blue), Model-4 (green) and Model-1 (dark yellow with $\tau_1 = 45º$ and grey with $\tau_1 = 0º$). Frequency calculations were performed at the M06-2X/6-31G(d,p) level of theory and the frequencies were scaled using a factor of 0.947. Lorentzian function, pitch = 1 cm^{-1}, fwhm (Full Width Half Maximum) = 4 cm^{-1}.

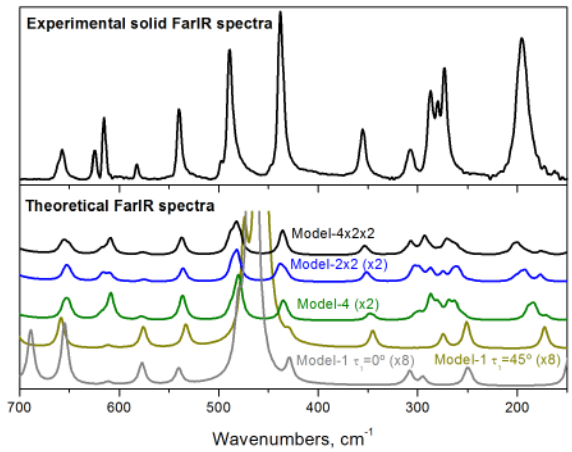

Figure 8. Experimental (upper) and predicted (lower) scaled FarIR spectra of **2PrBzIm**. Upper: Experimental FarIR spectrum of the powder sample. Lower: Theoretical FarIR spectra of Model-4x2x2 (black), Model-2x2 (blue), Model-4 (green) and Model-1 (dark yellow with $\tau_1 = 45º$ and grey with $\tau_1 = 0º$). Frequency calculations were performed at the M06-2X/6-31G(d,p) level of theory and the frequencies were scaled using a factor of 0.947. Lorentzian function, pitch = 1 cm^{-1}, fwhm (Full Width Half Maximum) = 4 cm^{-1}.

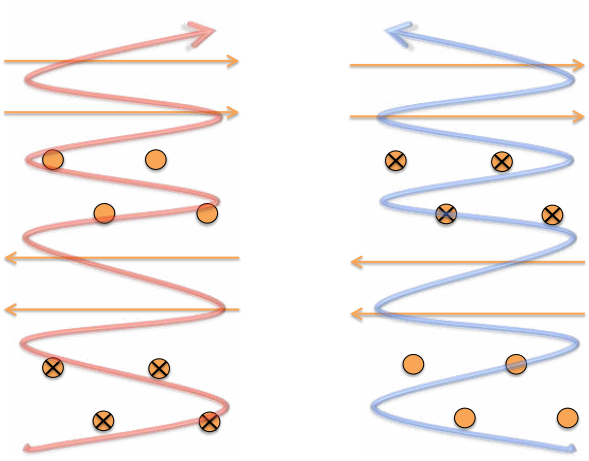

Figure 9. Schematic representation of the packing adopted by the two enantiomeric crystals expected from the crystal structure of **2PrBzIm**. The polarity of the molecular chains is represented by arrows towards right, left, up (circle) and down (cross).

3.3. Spectroscopic analysis using non-sensitive (IR, Raman) and sensitive (VCD) to chirality vibrational techniques

In Figure 8, a comparison of the theoretical and experimental FarIR spectra is shown. In this region, bands associated with normal modes with contributions from wagging, rocking and torsion modes are present. As above-mentioned, the Model-4x2x2 shows the best agreement with the experimental FarIR spectra, especially in the region below 350 cm^{-1}. Examples of these bands can be those observed at 306 cm^{-1}, which are assigned to CH_3 torsion and CH_3-CH_2-CH_2- bending normal modes, or the bands appearing at 287, 279 and 273 cm^{-1}, associated with CH_3 torsion and butterfly motions. A last example could be the band at 195 cm^{-1}, corresponding to imidazole and benzene rings breathing normal modes. In the literature, examples about how the assignments were made in similar situations can be found.[30,31]

In Figure 7, a good agreement between the experimental and theoretical IR and VCD spectra of **2PrBzIm** in nujol and fluorolube mulls is observed. The best theoretical models that match the experimental IR spectra are Model-2x2 and Model-4x2x2 and, in the case of the VCD spectra, the latter (as for FaIR spectra). If we focus our attention on the VCD spectra, there are a few key experimental bands that confirm the presence of a chiral structure and they are well reproduced from Model-4x2x2. Examples can be the (–) bands that appear in IR and VCD at 1621, 1540, 1479, 1469, 1450, 1436 and 1420 cm^{-1}. The first band (1621 cm^{-1}) is assigned to C=C str. and the second (1540 cm^{-1}), third (1479 cm^{-1}) and fourth (1469 cm^{-1}) to C-N-H bending normal modes, with the additional contribution in the third and fourth bands of ring deformations. The fifth (1450 cm^{-1}), the sixth (1436 cm^{-1}) and the seventh (1420 cm^{-1}) bands are associated with asymmetric CH_3 bending and CH_2 scissoring normal modes (see Table 2S ESI).

3.4. The invariance of the chirality.

VCD spectra of crystalline powders of commercial **2PrBzIm** sample were recorded in $CDCl_3$ solution and in fluorolube or nujol mulls (see Figure 10). Additionally, a selected summary of recorded VCD and IR spectra of samples of different recrystallizations origin is given in Figure 10 (SI for a complete dataset). The absent VCD spectrum of **2PrBzIm** in solution (Figure 10, dark

cyan) confirms the lack of chirality in **2PrBzIm** monomers or the rapid equilibrium between short chains (dimers, trimers).

All VCD spectra recorded for solid samples (mulls), however, displayed a consistent profile (Figure 10). Our first recorded VCD spectrum in solid phase was that of a commercial **2PrBzIm** sample without carrying out any recrystallization. The next VCD spectrum was recorded for a commercial sample recrystallized from a 3:1 Cl_2CH_2/hexane solvent mixture. These two VCD spectra showed the same chiroptical features. To understand whether or not the sample preparation had an effect on the enantiomeric purity (or excess) of the crystalline powders, we proceeded to repeat our second experiment four times through independent recrystallizations resulting always in the same VCD spectra. In addition, we recrystallized our purchased material from a variety of solvents ($CHCl_3$, Cl_2CH_2/hexane and acetone/water) and also recrystallized it from $CHCl_3$ using clockwise and anticlockwise stirring (Figure 10). We prepared samples by sublimation and we also obtained it through **2PrBzIm** hydrochloride by treating **2PrBzIm**·HCl with different bases. All samples gave identical VCD spectra, confirming either *homochirality* or *identical crystal enantiomeric excess* in all crystalline materials independently of the preparation method.

To rule out possible artifacts coming from the VCD spectrometer optics available in the University of Jaen (Jasco FVS-4000 FT-IR spectrometer), we recorded the VCD spectra of some **2PrBzIm** crystals using the FT-IR Bruker Vertex 70 spectrometer (with a PMA 50 module for VCD recordings) accessible at the University of Malaga (as mentioned in 2.2 section), resulting in the same chiroptical features than those previously obtained in our laboratory (see Figure 2S ESI).

Finally, another procedure was tested to get the opposite enantiomeric form (or the opposite enantiomeric excess, e.e.) of that observed for all the measured samples. It consisted in dissolving **2PrBzIm** in acetone and removing the solvent using a magnetic stirrer and a N_2 flow.[31] This methodology was successfully used by us in the case of two perfluorinated 1*H*-indazole derivatives of ref. 31. In the case of 3-(perfluoroethyl)-4,5,6,7-tetrafluoro-1*H*-indazole (YODJIM) and 3-(perfluoropropyl)-4,5,6,7-tetrafluoro-1*H*indazole (YODJOS), the opposite enantiomeric helices were obtained for both compounds by using the aforementioned procedure.[31] However, this was not successful for **2PrBzIm**, whose recorded VCD spectra were again the same than those obtained with all the methods previously described.

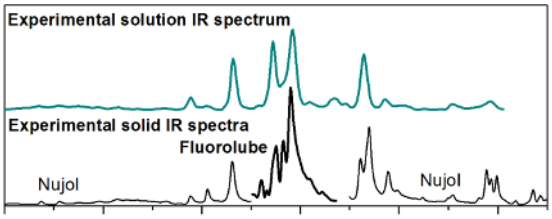

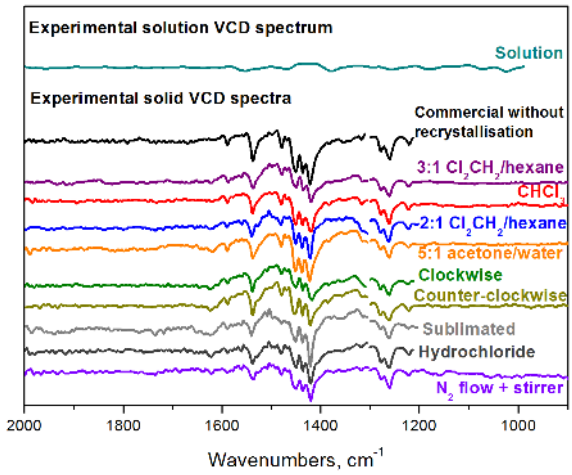

Figure 10. Recorded IR (upper) and VCD (lower) spectra for liquid (dark cyan) and solid samples (mulls) of **2PrBzIm**. Hydrochloride means a neutral sample obtained from the hydrochloride.

4. CONCLUSIONS

The structure and chirality of **2PrBzIm** in the solid state were studied in depth by a combination of X-ray crystallography, non sensitive (IR and Raman) and sensitive (VCD) chirality vibrational spectroscopies, and quantum chemical calculations.

We have discovered several new properties of the crystal structure of **2PrBzIm**; besides we have carried out many experiments trying to find the other enantiomer, some of them as rigorous as regenerating it from its salt, but with no success. We think it is important to report these findings even if they are contrary to the second principle of thermodynamics;[32] obviously a hidden source of optical activity, such as cryptochiral environment,[33] is present that we have not been able to identify. Note that, because our VCD experiments were carried out on powders, the Poeppelmeier discovery that single crystals of certain racemates show optical activity is not relevant for the present work.[34,35]

Whilst we have been able to rationalize the rare and subtle chirality arising from the crystal packing in this system, it remains a mystery why we always observe the same chiral response in this material. Despite both enantiomeric crystals being energetically identical and despite the subtle nature of the chiral origin, remarkably, we have obtained the same conglomerate independently of the origin of the sample and the crystallization method. Only a few authors have reported similar observations;[36,37,38,39,40] we hope that further reports of this kind may eventually lead to a scientific explanation for this enantiomeric selectivity. We suspect that the answers to these observations must lie in the nucleation[41] and growth mechanisms of the corresponding crystals; unfortunately, such an assertion is not possible in the light of our present knowledge of the subject. The production of enantiomerically enriched products from achiral precursors without the intervention of chiral chemical reagents or catalysts is known as "Absolute Asymmetric Synthesis".[42] Finally, note that **2PrBzIm** which is a simple compound, commercially available, stable, safe and easy to handle, constitutes an excellent model compound for further studies.

■ ASSOCIATED CONTENT

s **Supporting Information**

The Supporting Information is available free of charge on the ACS Publications website at DOI: 10.1021/acs.jpca.

1. Computational studies on 2PrBzIm: Table S1. Relative stability and relevant structural

parameters of the crystal structure of 2PrBzIm with *anti*, *syn* and mixed molecular configurations; 2. Symmetry operations of sub-structures Pcab and Pbca; 3. Results from COMPSTRU; 4. IR and VCD: 4.1. Experimental results: Figures S1a, S1c, S1d and S1e. Experimental IR and VCD spectra of the different commercial 2PrBzIm samples obtained through different methodologies; Figure S1b. Images of 2PrBzIm crystals obtained using a Renishaw Raman Microscope spectrometer (785 nm); Figure S2. Experimental VCD spectra of commercial 2PrBzIm crystals recorded using the VCD spectrometer available in Jaen (Jasco) and Malaga (Bruker); 4.2. Comparison between experiments and theory: Figures S3, S4, S5 and S6) Comparisons between FarIR, IR and VCD experimental and theoretical spectra of 2PrBzIm, showing the theoretical contribution of the three non-periodic models generated from the PBC optimized structure, that is, 4x2x2, 2x2 and 4 models for *anti* and *syn* configurations; Table S2. Experimental wavenumbers (cm^{-1}) of the most important observed bands in the FarIR, midIR and VCD spectra of 2PrBzIm and their assignment using the DFT-M062X/6-31G(d,p) level of theory.

AUTHOR INFORMATION

Corresponding Authors

*E-mail: rclaramunt@ccia.uned.es

*E-mail: jjlopez@ujaen.es (J.J.L.G.)

*E-mail: javier.zuniga@ehu.es (F.J.Z.)

ORCID

Notes

The authors declare no competing financial interest.

ACKNOWLEDGMENTS

The authors thank Francisco Hermoso Torres, Marina Gómez Torres, Cecilia Benítez Guerrero, Dr. Macarena López Sánchez, Dr. José Luis Zafra Paredes for technical assistance. The authors also thank the Universidad de Jaén for financial support, for bridge projects (UJA2015/08/07 and UJA2016/08/15) and access to its CICT instrumental facilities and they also thank the Universidad de Málaga for its SCAI instrumental facilities. This work was supported by Ministerio de Economía y Competitividad of Spain (CTQ2015-63997-C2-2-P and CTQ2014-56833-R), CICE/Junta de Andalucía (P08-FQM-04096), CICE/JA-FEDER-UJA: Plan de Fortalecimiento de las Capacidades de I+D+i/2014-15 (UJA2013/08/03), Comunidad Autónoma de Madrid (Project Fotocarbon, ref S2013/MIT-2841), by the Basque Government (IT779-13) and the Spanish MEC (FIS2010-19609-C02-01). M.M.Q.M. thanks the Universidad de Jaén for a predoctoral fellowship and J.R.A.M. thanks Junta de Andalucía for a post-doctoral grant.

REFERENCES

(1) Escande, A.; Lapasset, J. Les benzazoles (indazole, benzimidazole, benzotriazole) structure moléculaire et propriétés fondamentales. *Tetrahedron* **1974**, *30*, 2903–2909.

(2) Pérez-Torralba, M.; García, M. A.; López, C.; Torralba, M. C.; Torres, M. R.; Claramunt, R. M.; Elguero, J. Structural investigation of weak intermolecular interactions (hydrogen and halogen bonds) in fluorine-substituted benzimidazoles. *Cryst. Growth Des*. **2014**, *14*, 3499–3509.

(3) Cabildo, P.; Claramunt, R. M.; Zuñiga, F. J.; Alkorta, I.; Elguero, J. Crystal and molecular structures of two 1*H*-2-substituted benzimidazoles. *Z. Kristallogr*. **2015**, *230*, 427–438.

(4) García, M. A.; López, C.; Claramunt, R. M.; Kenz, A.; Pierrot, M.; Elguero, J. Polymorphism vs. desmotropy: the cases of 3-phenyl- and 5-phenyl-1*H*-pyrazoles and 3-phenyl-1*H*-indazole. *Helv. Chim. Acta* **2002**, *85*, 2763–2776.
(5) Teichert, J.; Oulié, P.; Jacob, K.; Vendier, L.; Etienne, M.; Claramunt, R. M.; López, C.; Pérez Medina, C.; Alkorta, I.; Elguero, J. The structure of fluorinated indazoles: the effect of the replacement of a H by a F atom on the supramolecular structure of NH-indazoles. *New J. Chem*. **2007**, *31*, 936–946.
(6) González, J. J. L.; Ureña, F. P.; Moreno, J. R. A.; Mata, I.; Molins, E.; Claramunt, R. M.; López, C.; Alkorta, I.; Elguero, J. The chiral structure of 1*H*-indazoles in the solid state: a crystallographic, vibrational circular dichroism and computational study. *New J. Chem*. **2012**, *36*, 749–758.
(7) Avilés-Moreno, J. R.; Quesada Moreno, M. M.; López González, J. J.; Claramunt, R. M.; López, C.; Alkorta, I.; Elguero, J. Self-assembly structures of 1*H*-indazoles in the solution and solid phases: a vibrational (IR, FIR, Raman, and VCD) spectroscopy and computational study. *ChemPhysChem* **2013**, *14*, 3355–3360.
(8) Santa María, D.; Claramunt, R. M.; Alkorta, I.; Elguero, J.; Zúñiga, F. J. The structure of 4,5,6,7-tetrafluoro-1*H*-benzotriazole in the solid state and in solution. *J. Fluor. Chem*. **2016**, *192*, 98–104.
(9) Santa María, D.; Claramunt, R. M.; Torralba, M. C.; Torres, M. R.; Alkorta, I.; Elguero, J. The structure and properties of 5,6-dinitro-1*H*-benzotriazole. *J. Mol. Struct*. **2016**, *1113*, 153–161.
(10) Estime, N.; Pena, R.; Teychené, S.; Autret, J. M.; Biscans, B. Characterization of the conglomerate form of acetyl-DL-leucine by thermal analysis and solubility measurements. *J. Cryst. Growth*. **2011**, *342*, 28–33.
(11) McLaughlin, D. T.; Nguyen, T. P. T.; Mengnjo, L.; Bian, C.; Leung, Y. H.; Goodfellow, E.; Ramrup, P.; Woo, S.; Cuccia, L. A. Viedma ripening of conglomerate crystals of achiral molecules monitored using solid-state circular dichroism. *Cryst. Growth Des*. **2014**, 14, 1067–1076.
(12) Lennartson, A.; Hedström, A.; Håkansson, M. Spontaneous generation of chirality in simple diaryl ethers. *Chirality* **2015**, *27*, 425–429.
(13) Kuroda, R.; Harada, T; Shindo, Y. A solid-state dedicated circular dichroism spectrophotometer: Development and application. *Rev. Sci. Instrum.* **2001**, *72*, 3802−3810.
(14) Merten, C.; Kowalik, T.; Hartwig, A. Vibrational Circular Dichroism spectroscopy of solid polymer films: Effects of sample orientation. *Appl. Spectrosc.* **2008**, *62*, 901−905.
(15) Buffeteau, T.; Lagugné-Labarthet, F.; Sourisseau, C. Vibrational circular dichroism in general anisotropic thin solid films: measurement and theoretical approach. *Appl. Spectrosc.*, **2005**, *59*, 732−745.
(16) Frisch, M. J.; Trucks, G. W.; Schlegel, H. B.; Scuseria, G. E.; Robb, M. A.; Cheeseman, J. R.; Scalmani, G.; Barone, V.; Mennucci, B.; Petersson, G. A. et al. *Gaussian 09, Revision D.01*; Gaussian: Wallingford CT, 2009.
(17) Zhao, Y.; Truhlar, D. G. The M06 suite of density functionals for main group thermochemistry, thermochemical kinetics, noncovalent interactions, excited states, and transition elements: two new functionals and systematic testing of four M06-class functionals and 12 other functionals. *Theor. Chem. Acc.* **2008**, *120*, 215–241.
(18) (a) Hariharan, P. C.; Pople, J. A. The influence of polarization functions on molecular orbital hydrogenation energies. *Theor. Chim. Acta* **1973**, *28*, 213–222. (b) Francl, M. M.; Pietro, W. J.; Hehre, W. J.; Binkley, J. S.; Gordon, M. S.; DeFrees, D. J.; Pople, J. A. Self-consistent molecular orbital methods. XXIII. A polarization-type basis set for second row elements. *J. Chem. Phys*. **1982**, *77*, 3654–3665.

(19) NIST Computational Chemistry Comparison and Benchmark DataBase (CCCBDB), Release 18, October 2016, Editor Russell D. Johnson III, (http://cccbdb.nist.gov).
(20) The Cambridge Structural Database, Groom, C. R.; Bruno, I. J.; Lightfoot, M. P.; Ward, S. C. *Acta Crystallogr. Sect B* **2016**, *72*, 171–179.
(21) Moss, G. P. Basic Terminology of Stereochemistry, International Union of Pure and Applied Chemistry, Organic Chemistry Division, IUPAC Recommendations 1996, *Pure & Appl. Chem.* **1996**, *68*, 2193–2222 and Preferred IUPAC Names, Chapter 9, September, **2004**, p. 33 (rule P-92.1.5.4).
(22) Hitchcock, P. B.; Hodgson, A. C. C.; Rowlands, G. J. The first examples of planar chiral organic benzimidazole derivatives. *Synlett* **2006**, 2625–2628.
(23) de la Flor, G.; Orobengoa, D.; Tasci, E.; Pérez-Mato, J. M.; Aroyo, M. I. Comparison of Structures applying the tools available at the Bilbao Crystallographic Center. *J. Appl. Crystallogr.* **2016**, *49*, 653–664.
(24) International Tables for Crystallography, vol. A, 6ª edition, 2016.
(25) Petricek, V., Dusek, M., Palatinus, L. Jana2006. Structure Determination Software Programs. Institute of Physics, Praha, Czech Republic, 2006.
(26) Macrae, C. F.; Bruno, I. J.; Chisholm, J. A.; Edgington, P. R.; McCabe, P.; Pidcock, E.; Rodríguez-Monge, L.; Taylor, R.; van de Streek, J.; Wood. P. A. Mercury CSD 2.0 - new features for the visualization and investigation of crystal structures. *J. Appl. Crystallogr.* **2008**, *41*, 466–470.
(27) Bernal, I.; Watkins, S. F. A list of organometallics kryptoracemates. *Acta Crystallogr. Sect. C* **2015**, *71*, 216–221.
(28) Fábián, L. and Brock, C. P. A list of organic kryptoracemates. *Acta Crystallogr. Sect. B* **2010,** *66***,** 94–103.
(29) Dryzun, C.; Avnir, D. On the abundance of chiral crystals. *Chem. Commun.* **2012**, *48*, 5874–5876.
(30) Quesada-Moreno, M. M.; Avilés-Moreno, J. R.; López-González, J. J.; Claramunt, R. M.; López, C.; Alkorta, I.; Elguero, J. Chiral self-assembly of enantiomerically pure (4*S*,7*R*)-campho[2,3-*c*]pyrazole in the solid state: a vibrational circular dichroism (VCD) and computational study. *Tetrahedron: Asymmetry* **2014**, *25*, 507–515.
(31) Quesada-Moreno, M. M.; Avilés-Moreno, J. R.; López-González, J. J.; Jacob, K.; Vendier, L.; Etienne, M.; Alkorta, I.; Elguero, J.; Claramunt, R. M. Supramolecular organization of perfluorinated 1*H*-indazoles in the solid state using X-ray crystallography, SSNMR and sensitive (VCD) and non sensitive (MIR, FIR and Raman) to chirality vibrational spectroscopies. *Phys. Chem. Chem. Phys.* **2017**, *19*, 1632-1643.
(32) Kondepudi, D.; Kapcha, L. Entropy production in chiral symmetry breaking transitions. *Chirality* **2008**, *20*, 524–528.
(33) Viedma, C. Selective chiral symmetry breaking during crystallization: parity violation or cryptochiral envirinment in control? *Cryst. Growth Comm*. **2007**, *7*, 553–556.
(34) Gautier, R.; Norquist, A. J.; Poeppelmeier, K. R. From racemic units to polar materials. *Cryst. Growth Des*. **2012**, *12*, 6267–6271.
(35) Gautier, R.; Klingsporn, J. M.; Van Duyne, R. P.; Poeppelmeier, K. R. Optical activity from racemates. *Nature Mat*. **2016**, *15*, 591–592.
(36) Cheung, P. S. M.; Gagnon, J.; Surprenant, J.; Tao, Y.; Xu, H.; Cuccia, L. A. Complete asymmetric amplification of ethylenediammonium sulfate using an abrasion/grinding technique. *Chem. Commun.* **2008**, 987–989.
(37) Azeroual, S.; Surprenant, J.; Lazzara, T. D.; Kocun, M.; Tao, Y.; Cuccia, L. A.; Lehn, J.-M. Mirror symmetry breaking and chiral amplification in foldamer-based supramolecular helical aggregates. *Chem. Commun.* **2012**, *48*, 2292–2294.

(38) Ziach, K.; Jurczak, J. Mirror symmetry breaking upon spontaneous crystallization from a dynamic combinatorial library of macrocyclic imines. *Chem Commun*. **2015**, *51*, 4306–4309.
(39) Lennartson, A.; Håkansson, M. Absolute asymmetric synthesis of five-coordinate complexes. *New J. Chem.* **2015**, *39*, 5936–5943.
(40) Gao, C.-Y.; Wang, F.; Tian, H.-R.; Li, L.-J.; Zhang, J.; Sun, Z.-M. Particular handedness excess through symmetry-breaking crystallization of a 3D cobalt phosphonate. *Inorg. Chem.* **2016**, *55*, 537–539.
(41) Davey, R. J.; Schroeder, S. L. M.; ter Horst, J. H. Nucleation of organic crystals - A molecular perspective. *Angew. Chem. Int. Ed.* **2013**, *52*, 2166–2179.
(42) Mislow, K. Absolute asymmetric synthesis: a commentary. *Coll. Czech. Chem. Commun*. **2003**, *68*, 849–864.